is counterintuitive to the conventional optical laws but it is totally consistent with the analysis based on the isofrequencies' for the channeled waves on anisotropic lattices discussed earlier.

In the conventional isotropic periodic structures, a unit cell is representative of the respective finite arrangement when the edge cells are terminated into the matched loads. However, the feature of *L-C* mesh to funnel power from a point source into the narrow beam leads to the question whether load impedances of the edge cells nonadjacent to the beam axis affect the channel formation and properties of the propagating waves. To explore this effect, the load impedances outside the vicinities of the source and the channel output cells were varied. A comprehensive analysis of finite BM simulated in ADS has shown that only the first three edge nodes at the channel axis contribute to the beam formation. These observations led us to the conclusion that the channels arising on the anisotropic *L-C* mesh are well confined and guide waves along their axes as predicted by isofrequencies. To further elucidate the mechanism of wave channeling, the lattice portions were progressively removed to retain the mesh only around the channel axis. These alterations of the mesh arrangement incurred no visible changes of the beam shape and intensity on the truncated grids. Thus, the simulation results have proved that the propagation channel formed on the *L-C* mesh is truly confined to a few cells at the channel axis. This property of the *L-C* mesh suggests that a number of independent channels with their own impedances and axis orientations could be formed on the grid. Since the channel directions vary with frequency and the unit cell parameters, the *L-C* mesh can act as a spatial frequency discriminator [2, 6] where each individual frequency is guided into a separate dedicated channel terminated in its own matched impedance at the mesh periphery.

4. CONCLUSIONS

It has been shown that 2D periodic meshes composed of *L-C* circuits collimate waves from a point source into beams. The beam directions are prescribed by the lattice symmetry and the admittance ratio $(Y_2/Y_1) < 0$. The basic properties of the channeled waves, determined by the isofrequencies, are invariant to the physical arrangements of the unit cells as long as the ratio (Y_2/Y_1) remains constant. Effect of the unit cell structure on the channeled wave propagation has been explored for the unit cell configurations composed of double series (SSM), double parallel (PPM), and mixed parallel-series (PSM) *L-C* circuits. Analysis of these meshes has shown that the type (forward or backward) of channeled wave can be altered in the designed frequency band by varying only capacitance in the mesh arms. These findings are of particular significance for implementation of tunable meshes used in beam steering and phase compensation applications.

Analysis of the channeled wave scattering at interfaces of dual *L-C* meshes showed that, in general, the "refracted" beams propagate only along the channel axes whose directions depend on the lattice parameters but not the angle of incidence onto interface.

REFERENCES

1. K.G. Balmain, A.A.E. Luttgen, and P.C. Kremer, Power flow for resonance cone phenomena in planar anisotropic metamaterials, IEEE Trans Antennas Propag 51 (2003), 2612–2618.
2. K.G. Balmain and A. Lüttgen, Using resonance cone refraction for compact RF metamaterial devices, In Proceedings of the International Conference on Electromagnetics in Advanced Applications, Torino, Italy, Sept. 2003, pp. 419–422.
3. E. Brennan, A. Gardiner, A. Schuchinsky, and V.F. Fusco, Waves in IEEE MTT-S International Microwave Symposium, Long Beach, CA, 2005; CD ROM Dig., TH3C-7.
4. A. Grbic and G.V. Eleftheriades, Negative refraction, growing evanescent waves, and sub-diffraction imaging in loaded transmission line metamaterials, IEEE Trans Microwave Theory Tech 51 (2003), 2297–2305.
5. A. Lai, C. Caloz, and T. Itoh, Composite right/left-handed transmission line metamaterials, IEEE Microwave Mag 5 (2004), 34–50.
6. E. Brennan, A. Gardiner, A. Schuchinsky, and V.F. Fusco, Real-time frequency spectrum analyser based on channel formation within L-C mesh metamaterials, In International Student Conference, St. Petersburg—Microwave Applications of Novel Physical Phenomena, Russia, Oct. 2005, pp. 111–113.
7. G.V. Eleftheriades and O.F. Siddiqui, Negative refraction and focusing in hyperbolic transmission-line periodic grids, IEEE Trans Microwave Theory Tech 53 (2005), 396–403.
8. R.A. Silin and V.P. Sazonow, Slow wave structures, National Lending Library for Science and Technology, Boston Spa, 1971 (Translation of Zamedliaiuschie sistemy, Moskva, 1966).

HIGH DIRECTIVITY IN LOW-PERMITTIVITY METAMATERIAL SLABS: RAY-OPTIC VS. LEAKY-WAVE MODELS

Giampiero Lovat,[1] Paolo Burghignoli,[2] Filippo Capolino,[3] and David R. Jackson[4]

[1] Department of Electrical Engineering
"La Sapienza" University of Rome
Via Eudossiana 18
00184 Roma, Italy
[2] Department of Electronic Engineering
"La Sapienza" University of Rome
Via Eudossiana 18
00184 Roma, Italy
[3] Department of Information Engineering
University of Siena
Via Roma 56
53100 Siena, Italy
[4] Department of Electrical and Computer Engineering
University of Houston
Houston, TX 77204-4005

Received 1 June 2006

ABSTRACT: *A study is presented on the directivity of grounded low-permittivity metamaterial slab structures that achieve highly directive broadside radiation. Two-dimensional (2D) configurations excited by electric line sources are considered, adopting a scalar plasma-like dispersive permittivity for the metamaterial medium that suitably models a wire medium in the presence of a 2D electromagnetic field, with the electric field directed along the wire axes. The role of leaky waves in producing the high directivity attainable with such structures is illustrated by comparing it with a simple ray-optic model for the radiation mechanism. We show how for increasing substrate heights, the leaky-wave effect (dominant for "optimal" thicknesses, and responsible for the very high directivity) evolves into a lensing effect purely explained with ray-optics, when losses are present.* © 2006 Wiley Periodicals, Inc.
Microwave Opt Technol Lett 48: 2542–2548, 2006; Published online in Wiley InterScience (www.interscience.wiley.com). DOI 10.1002/mop.22004

Key words: *leaky-wave antennas; leaky waves; metamaterials; planar antennas; wire medium*

1. INTRODUCTION

Grounded slabs made of artificial materials (metamaterials) with constitutive parameters exhibiting unusual properties are interesting candidates for planar antennas with enhanced radiative performance. In particular, since the early investigations of Gupta and co-workers, wire-medium slabs have been studied because of their capability to radiate narrow directive beams with simple sources [1–5]. It should be noted that in Ref. 6 the same geometry was analyzed to study the effect of an unwanted plasma layer over a magnetic source, reaching conclusions similar to those in Refs. 1–5. In Ref. 7 the radiation of a source in a metamaterial slab with a small positive permittivity has been compared with more standard Fabry-Perot cavity antennas.

As is well known, a wire medium can be described as an isotropic dielectric with a plasma-like dispersive permittivity for electromagnetic fields that propagate in the plane perpendicular to the wire axis and are polarized TM with respect to the wire axis [8–12]. The case of oblique incidence requires a more involved anisotropic spatially dispersive model [13]. In Ref. 5, a grounded low-permittivity slab has been studied with an electric line source as an excitation [Fig. 1(a)]. This configuration can produce a narrow beam at broadside, with an extremely high directivity. Conditions were derived for achieving maximum power density radiated at broadside, and the role of leaky waves in producing the enhanced broadside radiation and the narrow beam was demonstrated. A comparison with a low-permittivity half-space [Fig. 1(b)] was also provided in Ref. 5. Results showed that the half-space configuration could also provide a narrow beam, but not a significantly enhanced power density at broadside. It was also shown that for the half-space configuration the narrow beam is not due to a leaky mode, but is the result of a ray-optic lensing type of effect.

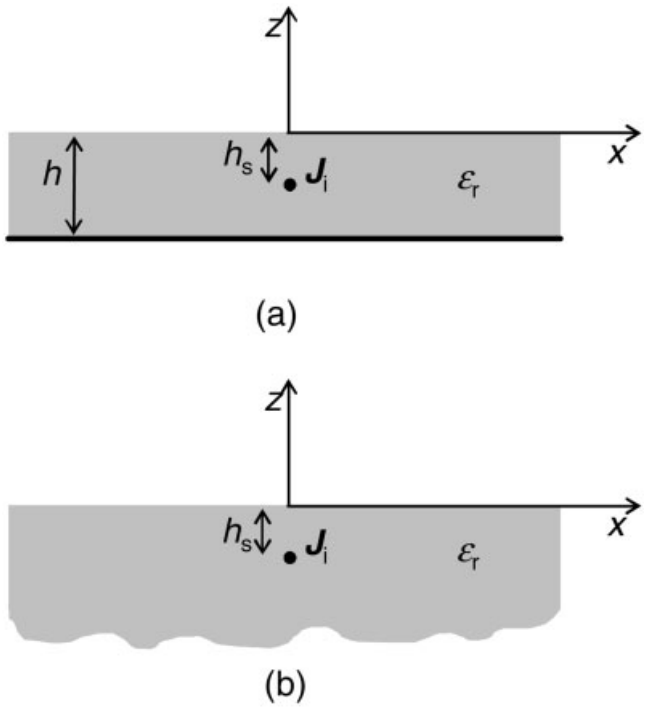

Figure 1 The low-permittivity structures considered here, with the relevant physical and geometrical parameters. (a) A grounded metamaterial slab with a line source inside. (b) A metamaterial half-space with a line source inside

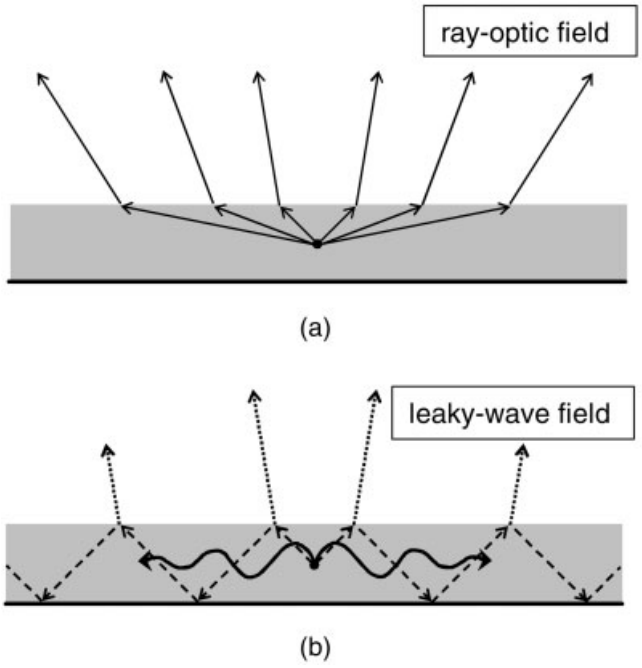

Figure 2 Radiation mechanisms for the highly directive broadside radiation attainable with the structure in Figure 1. (a) Ray-optic model showing the refractive lensing effect at the top interface. (b) Leaky-wave model showing a propagating leaky mode that is excited by the line source

There are two aspects that remain unclear: (a) the relative importance of the leaky-wave and ray-optic effects in producing the directivity enhancement for the slab problem, for both optimum and nonoptimum slab thicknesses, and (b) the manner in which the slab results approach that of the half-space as the slab thickness increases. An investigation of these aspects is the subject of the present letter.

2. RAY-OPTIC VS. LEAKY-WAVE MODELS

The frequency-dependent relative permittivity of a lossless plasma medium is

$$\varepsilon_r(f) = 1 - \frac{f_p^2}{f^2}, \tag{1}$$

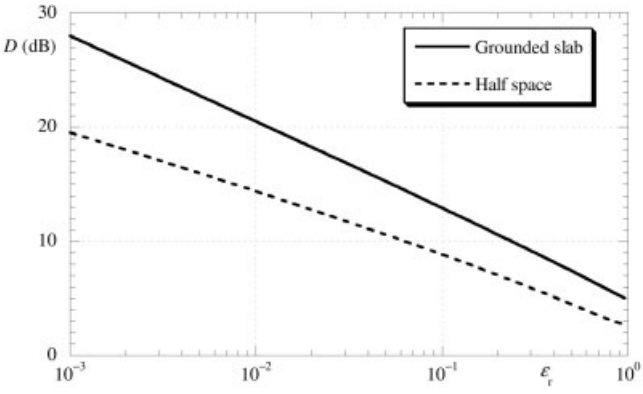

Figure 3 Directivity at broadside (in dB) as a function of the relative permittivity for an optimized grounded slab [Fig. 1(a), with $h = h_{opt}$) and for a half-space Fig. 1(b)]. In the two cases the same distance $h_s = h_{opt}/2$ of the electric line source from the air–metamaterial interface is assumed. In both cases the metamaterial is lossless

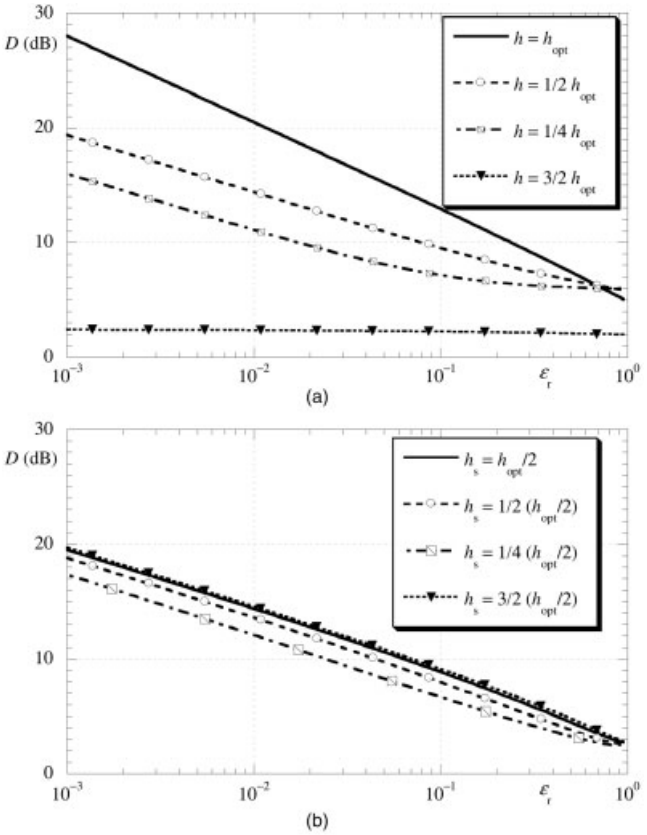

Figure 4 Directivity at broadside (in dB) as a function of the relative permittivity for (a) a lossless grounded slab with various thicknesses h and $h_s = h/2$, and (b) a lossless half-space with the same distances of the source from the air–metamaterial interface as in (a)

where f_p is the plasma frequency. This equation models well the effective relative permittivity of a wire medium when the electric field is parallel to the wires [8–12]. For $f > f_p$ (the "transparent" region) the effective relative permittivity is always positive and smaller than unity. Therefore, the rays emitted by a source placed inside a slab operating inside the transparent band will be refracted at the interface with a denser medium (e.g., air) with transmitted angles smaller than the critical angle $\theta_c = \sin^{-1}\sqrt{\varepsilon_r}$; this suggests a possible broadside directivity enhancement with respect to ordinary slabs. In Ref. 5 it was pointed out that, although very intuitive, this explanation captures only one aspect of the involved phenomenon and that a complete picture of the high-directivity effect can be obtained by considering the excited leaky-wave field (LWF) that propagates away from the source along the interface. In particular, the LWF can be thought as a wave field that consists of waves bouncing between the ground plane and the top interface; these waves add constructively when the slab has an optimum thickness to give maximum radiation at broadside, and such a constructive interference gives rise to an extremely directive broadside beam of radiation. A qualitative description of the two versions of the high-directivity phenomenon is sketched in Figure 2.

However, it still remains unclear how much of the overall directivity enhancement is actually due to the refraction at the top interface [which is the "ray-optic" effect in Fig. 2(a)] and how much of it is due to the constructive interaction between the two interfaces, which constitutes the leaky mode in Figure 2(b). Along the interface the LWF has the form

$$E_y^{\mathrm{LW}}(x) = A_{\mathrm{LW}} e^{-jk_{\mathrm{LW}}|x|}, \tag{2}$$

where $k_{\mathrm{LW}} = \beta - j\alpha$ [5]. For the plasma half-space there are no leaky waves [5] and the enhanced directivity is solely due to a ray-optic effect. In an effort to explore the importance of the leaky

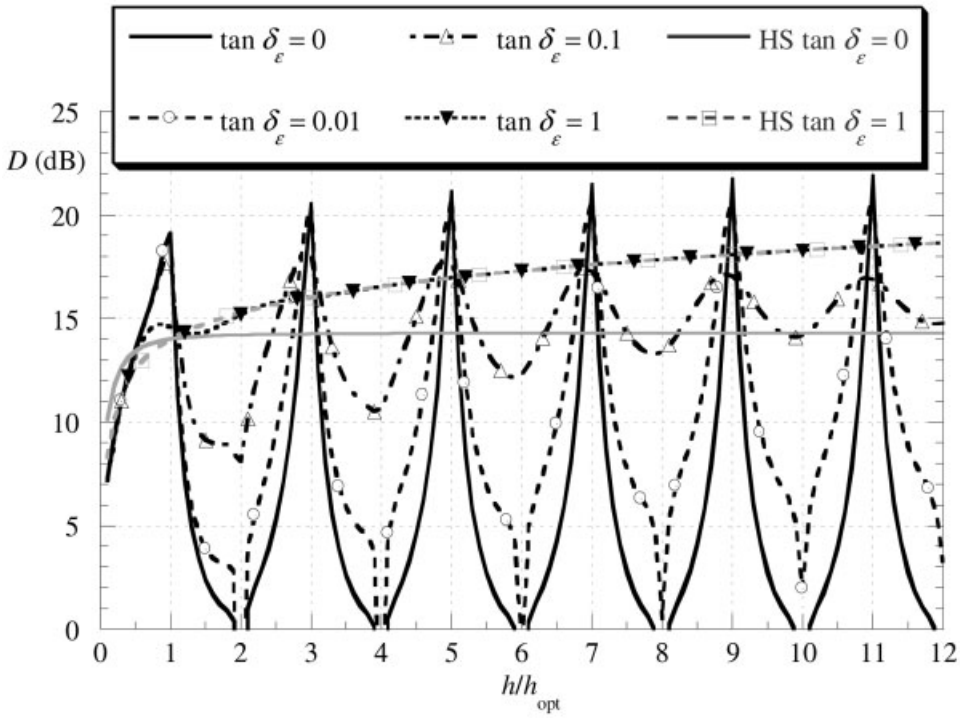

Figure 5 Directivity at broadside (in dB) as a function of the thickness h for a lossless grounded slab with $h_s = h/2$, for different values of the loss tangent. Also shown are results for lossless and lossy half-spaces, where the distance of the source from the interface is the same as for the slab. The optimum thickness $h_{\mathrm{opt}} = 59.2$ mm is chosen from Eq. (3) when $f = 1.008 f_p$ (this corresponds to $\varepsilon_r = 0.0158$)

wave versus ray optics, in Figures 3 and 4 we have calculated the directivities for two cases, a grounded plasma slab and a plasma half-space, with no losses.

In the 2D case of line-source excitation, the broadside directivity D is defined as

$$D = \frac{2\pi P(0)}{\int_{-\pi/2}^{\pi/2} P(\theta)\mathrm{d}\theta}, \tag{3}$$

where $P(\theta)$ is the radiated power density (power per unit angle). A comparison is made between the directivity of a line source in the middle of a plasma slab of thickness h and a line source at a distance h_s from the interface of a plasma half-space. To get a fair comparison, the distances from the line source to the top interface are the same in both cases so that $h_s = h/2$. Moreover, the slab thickness is chosen from the optimum condition that maximizes the broadside power density (and gives, approximately, the maximum directivity) [5] as

$$h = h_{\mathrm{opt}} \equiv \frac{\pi}{k_0\sqrt{\varepsilon_r}} = \frac{\lambda_\varepsilon}{2}, \tag{4}$$

where k_0 and λ_0 are the wavenumber and wavelength in free space and $\lambda_\varepsilon = \lambda_0/\sqrt{\varepsilon_r}$ is the wavelength inside the plasma slab. (With this optimum slab thickness, locating the source in the middle of the slab then maximizes the broadside power density.) More generally, the power density at broadside is maximized when the slab thickness is chosen as $h = nh_{\mathrm{opt}}$ for $n = 1,3,5,\cdots$. For even values of n the power density at broadside will be zero when the source is in the middle of the slab [5]; however, for other source locations ($h_s \neq h/2$) the values $n = 2,4,6,\cdots$ also produce a maximum power at broadside. The results are reported in Figure 3, where the directivity is compared between the slab and half-space configurations; in both cases the line source is at a distance $h_s = h_{\mathrm{opt}}/2$ from the top interface. The directivity of the half-space increases as the permittivity ε_r decreases, and this is due to the geometrical ray-optic effect that occurs at the top interface [Fig. 2(a)]. The directivity of the slab is significantly larger, however, and this is because of the constructive interference of multiple ray bounces within the slab, which constitutes the leaky mode. In particular, for smaller permittivities, the leaky-wave effect gives roughly an order of magnitude increase (more than 10 dB) in directivity compared with what the ray-optic effect alone produces. For the slab problem there is still a ray-optic effect, but the leaky-wave effect is dominant. For slab thicknesses that are not optimal, the leaky wave may become less important, and this is explored below.

The use of suboptimal thicknesses (i.e., $h < h_{\mathrm{opt}}$) reduces the value of the directivity significantly as can be seen in Figure 4(a), where different values of the slab thickness h are considered; the same occurs for slabs thicker than the optimum one (i.e., $h > h_{\mathrm{opt}}$). (The source is still at a distance $h_s = h/2$ from the interface in all cases.) In Figure 4(b) the corresponding changes in the directivity for the half-space configuration are reported for the same values of $h_s = 2h$ used in Figure 4(a). It is observed that the directivity monotonically increases as h (and thus h_s) increases for the half-space, but the effect of varying h on the directivity is much less compared to the effect observed in the slab problem. This is consistent with the physical mechanisms involved. In ray optics, an increase in h_s simply results in a larger effective aperture due to a geometrical lensing effect. For the slab structure, the leaky mode corresponds to a resonant constructive interference in the multiple wave bounces between the interface and the ground plane, and is thus critically dependent on the slab thickness h. Moreover, a significant difference can be observed for slabs that are thicker than the optimum one; in this case, the broadside directivity markedly decreases [Fig. 4(a)]. This rapid decrease in the broadside directivity as the slab thickness increases beyond the optimum thickness is due to the fact that the highly directive leaky-wave beam scans away from broadside towards the critical angle θ_c, as already observed in Ref. 5.

To get more information about the dependence of the directivity on the slab thickness, Figure 5 shows D as a function of the ratio h/h_{opt} (with the source placed at $h_s = h/2$) for different values of the loss tangent δ_ε; the optimal thickness h_{opt} is chosen from Eq. (3) when $f = 1.008f_p$ (this corresponds to $\varepsilon_r = 0.0158$). It can be seen that a "periodic" type of effect is present, and the broadside directivity has maxima corresponding to a odd multiple of the optimal thickness (each maximum corresponds to the optimal excitation of a successively higher-order leaky wave that radiates at broadside). The LWF is dominant for slab thicknesses close to the periodic optimal values $h = nh_{\mathrm{opt}}$ (n odd), thus giving rise to the high-directivity effect at broadside. It is less important for suboptimal slab thicknesses. This is verified in Figure 6(a), which shows that for suboptimal thicknesses $h < h_{\mathrm{opt}}$ the LWF decays much faster while the space-wave field

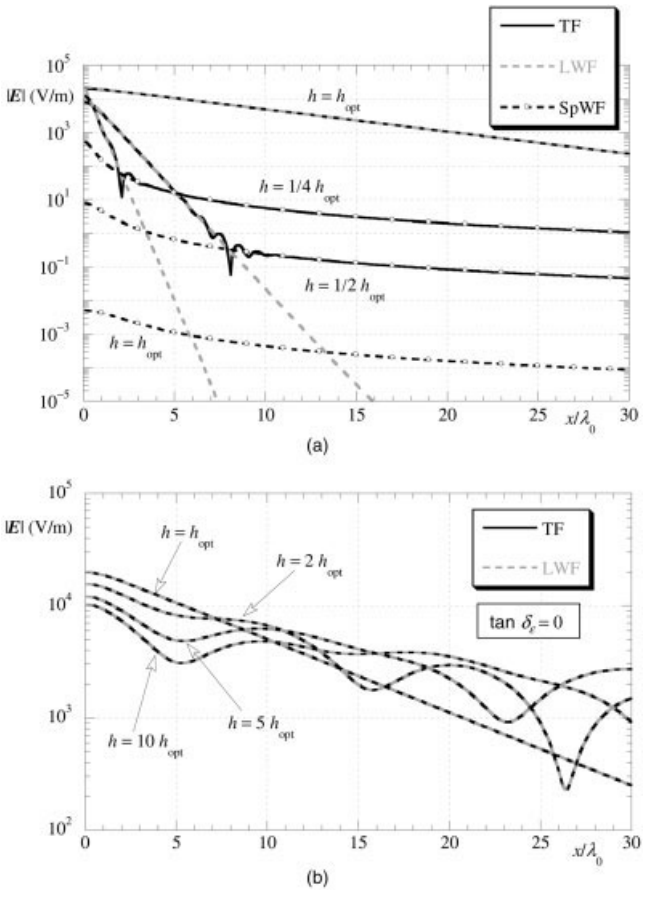

Figure 6 Amplitude of the electric field at the air–slab interface as a function of the normalized distance from the source x/λ_0 for different values of the slab thickness, for a lossless slab: (a) $h_s = h/2$ for $h \leq h_{\mathrm{opt}}$; (b) $h_s = h_{\mathrm{opt}}/2$ for $h \geq h_{\mathrm{opt}}$. TF: total field; LWF: leaky-wave field; SpWF: space-wave field. *Parameters*: $f_p = 20$ GHz, $f = 1.008f_p$ GHz, and $h_{\mathrm{opt}} = 59.2$ mm

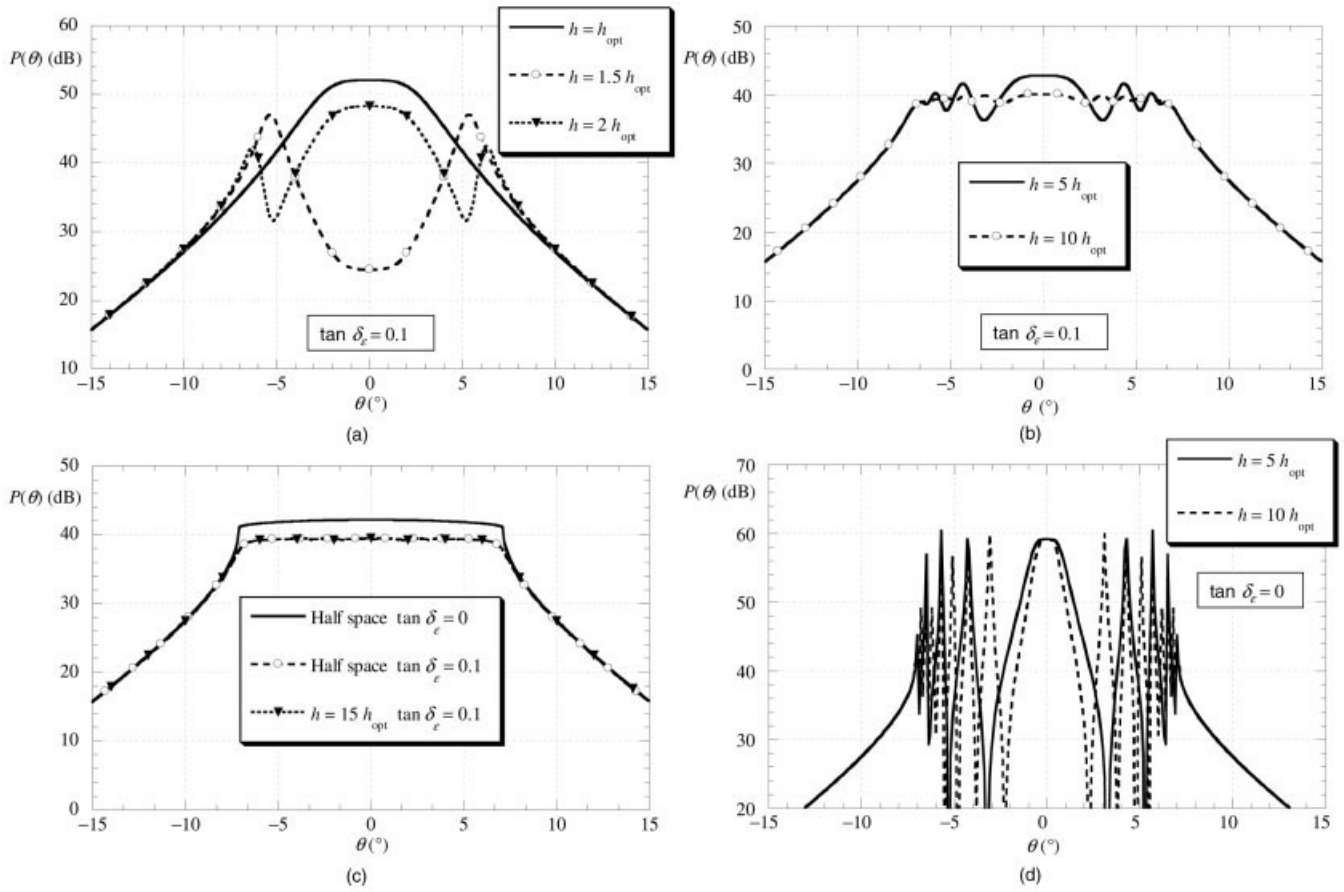

Figure 7 (a and b) Radiation patterns (in dB) for a lossy grounded slab (with parameters as in Fig. 6) with $\delta_\varepsilon = 0.1$ and different values of the slab thickness, when the source is placed at a fixed distance $h_s = h_{opt}/2$ from the slab–air interface. (c) Comparison between the radiation patterns of a lossy grounded slab as in (a) and (b) with $h = 15h_{opt}$, and corresponding lossless and lossy half-space problems (both structures have the source placed at a fixed distance $h_s = h_{opt}/2$ from the interface). (d) Same as in (b) but with tan $\delta_\varepsilon = 0$

(SpWF) becomes stronger. (The SpWF is defined as the residual field that is left over when the LWF is subtracted from the total field (TF). Far away from the source, this field decays asymptotically as $|x|^{-3/2}$ [14, Chap. 5]. By adding loss, the periodic fluctuations in Figure 5 decrease, since the multiple bounces within the slab that constitute the LWF are more attenuated as the slab thickness increases. In the lossy case the directivity should approach that of the half-space as the thickness increases, as is clearly visible in the tan $\delta_\varepsilon = 1$ case of Figure 5. Also the curve tan $\delta_\varepsilon = 0.1$ is beginning to exhibit this behavior (although convergence to a limiting value occurs for thicknesses off the scale of the plot).

To determine how the use of nonoptimal slab thicknesses affects the dominant role of the LWF, a comparison between the exact total field, the LWF, and the SpWF is presented in Figure 6. In particular, the amplitude of the corresponding electric fields at the air–slab interface is reported as a function of the normalized distance from the source for a structure as in Figure 1 with $f_p = 20$ GHz at the frequency $f = 1.008f_p$, for which $\varepsilon_r = 0.0158$ and $h_{opt} = 59.2$ mm mm. (This structure is the same as that considered in Ref. 5, where the calculation of the constituents of the electric field has also been explained.) It can be seen that, as expected, for $h = h_{opt}$ the LWF is completely superimposed to the TF, thus revealing its dominant character over a large portion of the interface. For slab thicknesses smaller than h_{opt} [Fig. 6(a)] the contribution of the SpWF becomes more important as the slab thickness becomes smaller than h_{opt}. For slab thicknesses larger than h_{opt} [Fig. 6(b)] the TF is still superimposed to the LWF, which is now oscillating because of the interference between all the leaky waves that have been excited. In particular, as n increases in the formula $h = nh_{opt}$ an increasingly higher-order leaky wave is responsible for the directive beam at broadside, while the lower-order leaky waves are still present in increasing numbers.

In Figure 7, it can be observed how the far-field radiation pattern of a line source inside a lossy grounded plasma slab (with parameters as in Fig. 6) evolves into the one produced by the same source inside the corresponding lossy plasma half-space. The loss tangent is tan $\delta_\varepsilon = 0.1$. Different thicknesses $h > h_{opt}$ of the slab are considered, when the source is placed at a distance $h_k = h_{opt}/2$ from the interface. In Figure 7(a) it can be seen that for the optimum thickness ($h = h_{opt}$) the beam points exactly at broadside; by increasing the slab thickness to $h = 1.5h_{opt}$ the beam scans from broadside towards the critical angle (θ_c 7.1°). By further increasing the slab thickness to $h = 2h_{opt}$, the beam has nearly reached the critical angle, while a higher-order leaky wave has begun to radiate at broadside. As the slab thickness increases still further [Fig. 7(b)] additional peaks (due to higher-order leaky waves) emerge, although the amplitude of the pattern oscillation decreases due to the loss. Eventually, for very thick slabs ($h = 10h_{opt}$) the pattern oscillation dies out and the pattern begins to become smooth. For $h = 15h_{opt}$ [Fig. 7(c)] the pattern has become quite smooth, and it is seen from Figure 7(c) that it is almost coincident with the pattern of the line source inside the corresponding lossy half-space (keeping the same distance of the source

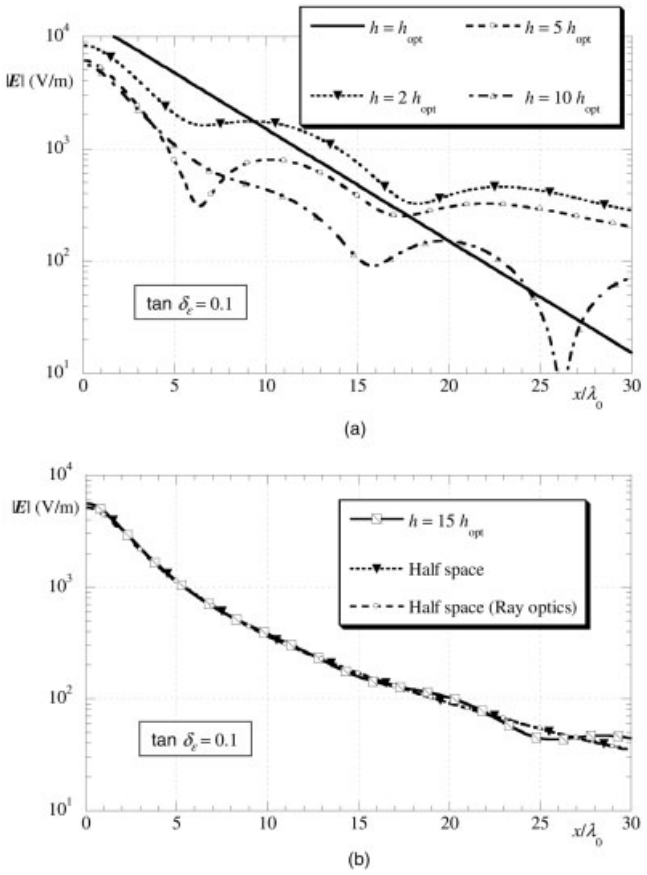

Figure 8 Amplitude of the electric field at the slab–air interface: (a) as a function of the normalized distance from the source x/λ_0 for the lossy grounded slab of Figures 7(a) and 7(b), for different values of the slab thickness h, with $h_s = h_{opt}/2$. (b) Comparison of this field with that existing at the interface in the corresponding half-space problem (having the same distance $h_s = h_{opt}/2$ between the source and the interface). For the half-space problem, the field at the interface that is predicted by ray optics is also shown for comparison

from the interface, $h_s = h_{opt}/2$). Figure 7(c) also shows that the pattern of the source inside the lossy half-space is not that different from the corresponding pattern for the lossless half-space, which is to be expected since the loss is not that large.

In Figure 7(d) the same radiation patterns are shown, as in Figure 7(b), but for a lossless slab. It is seen that in the absence of loss, the pattern for a thick slab becomes wildly oscillating with many sharp peaks, due to the higher-order leaky waves. Each excited leaky wave produces a peak that is confined to the angular region $-\theta_c < \theta < \theta_c$. Increasing the slab thickness increases the number of peaks in the region $-\theta_c < \theta < \theta_c$. The effect of loss smoothes out the radiation from the sum of leaky waves and produces the "plateau" pattern in Figure 7(c).

Figure 7 thus shows how the pattern changes from a leaky-wave type of pattern that is rapidly oscillating to a "lens" type of pattern (which is almost constant out to the critical angle, and almost zero beyond), as the slab thickness increases, provided there is some loss. In the completely lossless case, the slab pattern never approaches that of the half-space, and becomes increasingly oscillatory as the thickness increases, due to the higher-order leaky waves.

Figure 8 shows the amplitude of the electric field at the air–plasma interface for the same structures considered in Figure 7, as a function of the normalized distance from the source for the same values of h considered in Figure 7. When $h = h_{opt}$, Figure 8(a) shows that the interface field in the lossy grounded slab problem is almost entirely due to the dominant leaky wave, and is thus exponentially decaying (a straight line on the log scale). The field is significantly different from the total field of the lossy half-space problem. However, for larger values of h, the lossy grounded-slab and the lossy half-space interface fields are more alike. For $h = 15h_{opt}$, Figure 8(b) shows that the aperture fields of the lossy slab and half-space have become essentially the same. This is consistent with the behavior of the radiation patterns observed in Figure 7(c).

The field on the half-space interface can be approximated quite accurately by using a ray-optic formulation, as shown by the comparison between the exact interface field and the ray-optic approximation, included in Figure 8(b). The latter is evaluated as the incident field of the line source (with the Hankel function approximated by its first-order asymptotic expansion) multiplied by the Fresnel plane-wave transmission coefficient at the interface.

It is very reasonable that the ray-optic field accurately describes the exact interface field when the source distance h_s is large and the distance x from the source along the interface is not too large compared with h_s. However, it is less clear how well the ray-optic result should agree with the exact interface field for extreme distances x. An asymptotic analysis of the half-space problem (omitted here) shows that the interface field can be expressed as the sum of two terms, arising from steepest-descent integrations from the branch points at $k_1 = k_0\sqrt{\varepsilon_r} = 2\pi/\lambda_c$ and k_0 in the complex k_x plane [14, p. 321]. (We are assuming $x\ h_s$ so that the steepest-descent paths are vertical lines starting from the two branch points.) Both fields decay asymptotically along the interface as $|x|^{-3/2}$. An asymptotic evaluation of the wave arising from the k_0 branch point under the assumption that $x\ h_s$ yields a result that mathematically approaches the field along the interface predicted by ray optics, provided the source distance h_s becomes large. The wave arising from the k_0 branch point is one that is commonly referred to as a "lateral wave" [14, p. 308]. An asymptotic evaluation of this wave shows that the amplitude of the corresponding interface field is exponentially small as the source distance h_s increases. Hence, as the source height increases, the lateral-wave field on the interface is negligible, and the correct asymptotic evaluation of the interface field coincides with the ray-optic result.

Hence, it is not surprising that such good agreement is seen in Figure 8(b) between the exact interface field and that predicted by the ray-optic formulation throughout the entire range of values shown for the distance x along the interface, including both small and large values of x.

3. CONCLUSIONS

A low-permittivity grounded metamaterial slab with a line source inside can be used to obtain a highly directive beam at broadside. When the structure is properly optimized ($h = h_{opt}$), the directive broadside radiation is mainly due to a single leaky wave that is excited by the source. However, when $h < h_{opt}$, the directivity decreases and the role of the leaky wave becomes less important. For larger slab thicknesses ($h > h_{opt}$) multiple leaky waves are always important when the slab is lossless, and produce multiple directive beams that are confined to an angular region between broadside and the critical angle. This results in an overall pattern that is wildly oscillating. For a slab that has some loss, the oscillations die out and the pattern stabilizes as the slab thickness increases. The pattern and directivity then approach that of the corresponding lossy half-space (assuming that the distance from

the source to the interface remains the same in both problems). This half-space pattern is a "lens" type of pattern, which is nearly constant out to the critical angle, and rapidly decaying beyond. This lens type of pattern shows a directivity enhancement relative to the same source in free space, although the directivity is not as large as it is for an optimized lossless slab. Furthermore, the directivity enhancement for the half-space configuration is due solely to a ray-optic effect, and not a leaky wave.

REFERENCES

1. K.C. Gupta, Narrow-beam antennas using an artificial dielectric medium with permittivity less than unity, Electron Lett 7 (1971), 16–18.
2. I.J. Bahl and K.C. Gupta, A leaky-wave antenna using an artificial dielectric medium, IEEE Trans Antennas Propag 22 (1974), 119–122.
3. G. Poilasne, P. Pouliguen, J. Lenormand, K. Mahdjoubi, C. Terret, and P. Gelin, Theoretical study of interactions between antennas and metallic photonic bandgap materials, Microwave Opt Technol Lett 15 (1997), 384–389.
4. S. Enoch, G. Tayeb, P. Sabouroux, N. Guerin, and P. Vincent, A metamaterial for directive emission, Phys Rev Lett 89 (2002), 213902–1–213902–4.
5. G. Lovat, P. Burghignoli, F. Capolino, D.R. Jackson, and D.R. Wilton, Analysis of directive radiation from a line source in a metamaterial slab with low permittivity, IEEE Trans Antennas Propagat 54 (2006), 1017–1030.
6. T. Tamir and A.A. Oliner, The influence of complex waves on the radiation field of a slot-excited plasma layer, IRE Trans Antennas Propag 10 (1962), 55–65.
7. G. Lovat, P. Burghignoli, F. Capolino, and D.R. Jackson, Highly-directive planar leaky-wave antennas: A comparison between metamaterial-based and conventional designs, EuMA (European Microwave Association) Proceedings, in press.
8. J. Brown, Artificial dielectrics having refractive indices less than unity, Proc IEEE 100 (1953), 51–62.
9. W. Rotman, Plasma simulation by artificial dielectrics and parallel-plate media, IRE Trans Antennas Propag 10 (1962), 82–95.
10. J.B. Pendry, A.J. Holden, W.J. Stewart, and I. Youngs, Extremely low frequency plasmons in metallic mesostructures, Phys Rev Lett 76 (1996), 4773–4776.
11. J.B. Pendry, A.J. Holden, D.J. Robbins, and W.J. Stewart, Low frequency plasmons in thin-wire structures, J Phys: Condens Matter 10 (1998), 4785–4809.
12. P.A. Belov, S.A. Tretyakov, and A.J. Viitanen, Dispersion and reflection properties of artificial media formed by regular lattices of ideally conducting wires, J Electromag Waves Appl 16 (2002), 1153–1170.
13. P.A. Belov, R. Marquès, S.I. Maslovski, M. Silveirinha, C.R. Simovski, and S.A. Tretyakov, Strong spatial dispersion in wire media in the very large wavelength limit, Phys Rev B: Solid State 67 (2003), 113103–1–113103–4.
14. L.B. Felsen and N. Marcuvitz, Radiation and scattering of waves, IEEE Press, Piscataway, NJ, 1994.

VERIFICATION OF IMPEDANCE MATCHING AT THE SURFACE OF LEFT-HANDED MATERIALS

Koray Aydin,[1,2] Irfan Bulu,[1,2] and Ekmel Ozbay[1–3]
[1] Nanotechnology Research Center
Bilkent University
Bilkent, Ankara 06800 Turkey
[2] Department of Physics
Bilkent University
Bilkent, Ankara 06800 Turkey
[3] Department of Electrical and Electronics Engineering
Bilkent University
Bilkent, Ankara 06800 Turkey

Received 2 June 2006

ABSTRACT: *Impedance matching at the surface of left-handed materials (LHM) is required for certain applications including a perfect lens. In this study, we present the experimental and theoretical verification of an impedance-matched LHM to free space. Reflection characteristics of both one-dimensional and two-dimensional LHM were investigated. The reflection was observed to be very low at a narrow frequency range. FDTD simulations and retrieval procedures were used to theoretically verify impedance matching. By varying the number of layers along the propagation direction, the ultralow reflection at specific frequencies was shown to be independent of the sample thickness.* © 2006 Wiley Periodicals, Inc. Microwave Opt Technol Lett 48: 2548–2552, 2006; Published online in Wiley InterScience (www.interscience.wiley.com). DOI 10.1002/mop.22003

Key words: *left-handed materials; metamaterials; reflection; impedance matching; perfect lens*

1. INTRODUCTION

Materials that possess a negative index of refraction have become a remarkable research area in recent years because of their interesting properties and novel applications. The intriguing physics of a medium having a negative refractive index was discussed by Veselago theoretically nearly four decades ago [1]. Veselago predicted that a medium with simultaneous negative permittivity along with negative permeability exhibits unusual physical properties; among them are negative refraction, reversal of Doppler shift, and backward Cerenkov radiation. In the pioneering work of Pendry et al., a metallic thin wire grid was shown to exhibit a plasma frequency in the microwave regime, below which the effective permittivity takes negative values [2]. Thereafter, a split-ring resonator (SRR) structure is proposed to have $\mu(\omega) < 0$ near the magnetic resonance frequency [3]. Experimental realization of left-handed metamaterials (LHM) was achieved by arranging $\varepsilon(\omega) < 0$ media and $\mu(\omega) < 0$ media periodically [4, 5]. A left-handed transmission band was observed at the frequencies where both ε and μ are negative. This was later followed by the direct measurement of a negative refractive index by means of different methods [6–8]. Recent experimental and theoretical studies have reported the exotic electromagnetism of LHMs, such as negative phase velocity [7, 9], backward wave radiation [10], and perfect lens behavior [11]. Special interest was given to the perfect lens phenomena where the amplitude of evanescent waves are restored, enabling the so-called subwavelength focusing. Aydin et al. recently reported subwavelength focusing by using a LHM flat lens [12]. Most of the experimental measurements on LHMs are performed on microwave frequency region; but there is a tendency to increase the operation frequency up to terahertz [13, 14] and even optical frequencies [15].